

Northumbria Research Link

Citation: Perera, Dilini, Upasiri, Irindu, Poologanathan, Keerthan, Perampalam, Gatheeshgar, O'Grady, Kate, Rezazadeh, Mohammadali, Rajanayagam, Heshachanaa and Hewavitharana, Thatssarani (2022) Fire performance analyses of modular wall panel designs with loadbearing SHS columns. *Case Studies in Construction Materials*, 17. e01179. ISSN 2214-5095

Published by: Elsevier

URL: <https://doi.org/10.1016/j.cscm.2022.e01179>
<<https://doi.org/10.1016/j.cscm.2022.e01179>>

This version was downloaded from Northumbria Research Link:
<http://nrl.northumbria.ac.uk/id/eprint/49245/>

Northumbria University has developed Northumbria Research Link (NRL) to enable users to access the University's research output. Copyright © and moral rights for items on NRL are retained by the individual author(s) and/or other copyright owners. Single copies of full items can be reproduced, displayed or performed, and given to third parties in any format or medium for personal research or study, educational, or not-for-profit purposes without prior permission or charge, provided the authors, title and full bibliographic details are given, as well as a hyperlink and/or URL to the original metadata page. The content must not be changed in any way. Full items must not be sold commercially in any format or medium without formal permission of the copyright holder. The full policy is available online: <http://nrl.northumbria.ac.uk/policies.html>

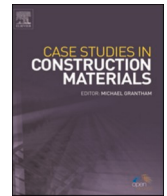
This document may differ from the final, published version of the research and has been made available online in accordance with publisher policies. To read and/or cite from the published version of the research, please visit the publisher's website (a subscription may be required.)



ELSEVIER

Contents lists available at [ScienceDirect](https://www.sciencedirect.com)

Case Studies in Construction Materials

journal homepage: www.elsevier.com/locate/cscm

Fire performance analyses of modular wall panel designs with loadbearing SHS columns

Dilini Perera^{a,*}, I.R. Upasiri^b, K. Poologanathan^a, Gatheeshgar Perampalam^c,
Kate O'Grady^d, Mohammadali Rezazadeh^a, H. Rajanayagam^a,
Thathsarani Hewavitharana^e

^a Faculty of Engineering and Environment, Northumbria University, Newcastle upon Tyne, UK

^b Department of Civil Engineering, University of Sri Jayawardenepura, Sri Lanka

^c School of Computing, Engineering & Digital Technologies, Teesside University, UK

^d ESS Modular, Crag Ave, Clondalkin Industrial Estate, Dublin 22, Ireland

^e Department of Civil Engineering, Faculty of Engineering, University of Moratuwa, Sri Lanka

ARTICLE INFO

Keywords:

Loadbearing modular walls
Square Hollow Section
Structural FRL
Load Ratio
Insulation Ratio
Heat Transfer Analyses

ABSTRACT

Modular Building Systems (MBS) are still in the phase of developing its popularity in the industry, with emerging novel designs. Initially, MBS walls and floors had been highly influenced by the Light-gauge Steel Frame (LSF) designs made of Cold-Formed (CF) steel studs, either as load-bearing or non-loadbearing types which have been extensively researched all over the world. However, recently the MBS practice in the industry tends to incorporate Square Hollow Section (SHS) steel columns for their improved structural performance and convenience at the manufacturing stage despite of the limited research knowledge in terms of the Fire Resistance Level (FRL). Moreover, catastrophic failures and fatal accidents are common with steel-based structures in case of a fire. Hence, the fire performance of loadbearing modular walls with SHS columns have been identified as a critical research gap. Firstly, Finite Element Models (FEM) were developed for the original modular wall, a Light-weight Timber Frame (LTF) wall and some LSF walls. The FEM analyses results very well matched with the full-scale experimental results so that the FEM techniques were confidently used to study the effect of variables chosen based on material availability options, cost reduction and construction practice. Structural and Insulation FRLs have been evaluated for the chosen parametric walls, where the produced graphs of structural and insulation FRLs can be referred to determine the adequate thickness of column sheathing and the Insulation Ratio (IR) respectively. The choice of non-loadbearing stud type can be evaluated against other limitations related to energy, cost and construction practice.

1. Introduction

1.1. Background

Light-gauge Steel Frame (LSF) techniques, and Modular Building Systems (MBS) are identified as the most prominent and still

* Corresponding author.

E-mail address: dilini.perera@northumbria.ac.uk (D. Perera).

<https://doi.org/10.1016/j.cscm.2022.e01179>

Received 24 March 2022; Received in revised form 13 May 2022; Accepted 17 May 2022

Available online 21 May 2022

2214-5095/© 2022 The Author(s). Published by Elsevier Ltd. This is an open access article under the CC BY license (<http://creativecommons.org/licenses/by/4.0/>).

evolving methods in the construction industry. In comparison to the traditional practices, these techniques have significantly relieved the stresses in the industry. More specifically, the options of pre-fabrication and mass scale production in factory environments have eased the situation against skilled labour shortage, time restraints, material scarcity, financial restraints, waste minimisation requirements and the high-quality assurance demanded by continuously updating rules and regulations. Generally, the conventional LSF construction practice is to prefabricate LSF wall, ceiling, and floor panels separately at the factory manufacturing stage followed by the foundation work, assembling of walls, floor and ceilings, Mechanical, Electrical and Plumbing (MEP) duties and the finishes at the construction site. Therefore, conventional LSF practice was still demanding a significant workload to be carried out at the construction site. On the other hand, MBS practice is referred to as prefabrication of whole volumetric modular units, followed by the MEP and finishing work also at the factory manufacturing stage so that much reduced work is left to be carried out at the construction site. Hence, MBS practice exhibits even more attractive advantages with respect to the conventional LSF construction.

The state of the art of LSF and MBS technologies, has been evolving throughout the whole time producing innovative wall and floor panels ensuring more and more efficient solutions in terms of structural, energy and fire performances although construction time reduction, labour demand reduction, cost cutting, material availability and the convenience seem to be the prime driving factors on these changes. Therefore, research investigation on these continuously updating LSF and MBS building components is always welcome. In fact, structural performance, Fire Resistance Levels (FRL) and energy efficiency are the basic research scopes that need to be addressed of any emerging construction practice or any novel building component design.

Commonly, conventional and modular LSF wall panel designs consist of Lipped Channel Section (LCS) or channel section Cold-Formed (CF) steel studs, rockwool/ glass fibre/ mineral wool insulation material and fire-resistant wall boards such as Gypsum plasterboards or Calcium Silicate boards. The integrated CF steel studs are designed for compression load where the wall panels are meant to be loadbearing walls. The possibility is also there for these conventional or modular LSF wall panels to be non-load bearers where the corner-supporting frame structure is designed to withstand the structural load applied. Here the former type of walls will form four sided modules and the latter will form corner supported modules when MBS designs are concerned as per Liew et al. [1]. The typical LSF wall designs with LCS and channel section studs shown in Fig. 1, have been widely addressed by the recent research studies against their structural and fire performance. For instance, studies of LSF wall systems carried out with respect to stud geometry [2–4], cavity insulation type [5–7], the location of insulation material [8], sheathing option [9–11] and the amount of integrated cavity insulation [12] are few recent research studies that have addressed the structural and fire performance research scopes. Studies on overall structural-fire failure of cold-formed steel buildings [13] and modular floor panels [14] have even influenced the research understanding to the scope. Furthermore, LSF wall panel energy efficiency has been identified as a key research gap and hence, it is being researched considering the LSF wall panels with LCS and channel section studs against European practices and climate conditions [15–18].

1.2. Research focus

Although channel section steel stud applied in LSF walls had been a quite popular design in the previous decade, due to the susceptibility of buckling failure and lower compression load carrying capacity, these LSF wall designs were generally supposed to be non-loadbearing walls even in a two-story construction. Therefore, even for a low to mid rise MBS construction, the necessity of structural load supporting frame structure had been inevitable. With the objectives of minimising the construction time, labour demand at the construction site and for the convenience, the European industry has been transforming the modular wall panel designs integrating

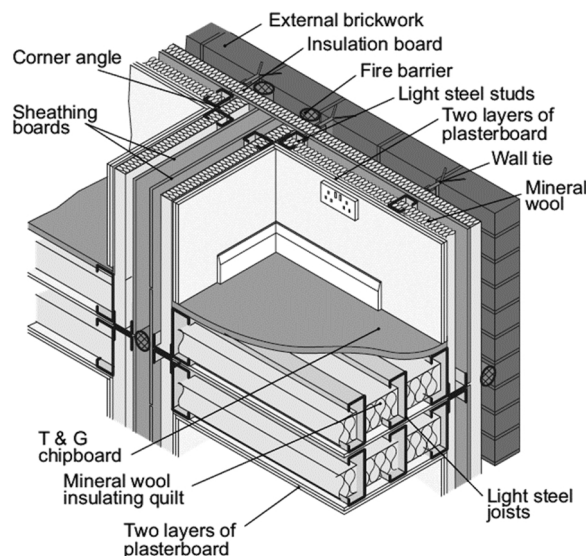


Fig. 1. Assembly of modular walls and floors designed with LCS studs [19].

Square Hollow Section (SHS) steel columns. One such loadbearing modular wall panel design is shown in Fig. 2 that has been experimented by Yu et al. [20].

This wall panel consists of loadbearing $90 \times 90 \times 6$ SHS steel columns sheathed with 32 mm thick gypsum plasterboards, non-loadbearing 60x40x3 Rectangular Hollow Section (RHS) steel studs located at 400 mm and 415 mm centres, mineral wool thermal cavity insulation and 9 mm thick gypsum plasterboards as the wall panel sheathing. Despite the new trends in the construction industry regarding the modular wall panels with SHS load bearers, research studies addressing structural, fire and energy performance criteria are still being very limited. Hence, the wall panel designs currently practiced in the industry are overdesigned and a number of experimental and numerical research and investigation studies are necessary to optimise the SHS section applied modular wall panels ensuring adequate structural, fire and energy performances. Setting out the objectives to optimise the modular wall panel design in Fig. 2, as an initial step to explore the described research scopes, the current study aims to conduct a parametric study based on the original modular wall panel design along with other material options available in the European construction industry. Specifically, this study is based on the influence of non-loadbearing stud type, thickness of plasterboard sheathing of loadbearing SHS columns, and cavity insulation ratio for the structural and fire performance of the modular wall panel.

2. Determination of Fire Resistance Level

2.1. Standard practice

Eurocode 3: Part 1-2 [21], the most prominent code of practice followed in the region on the structural fire designing has been referred when determining the FRL of the original and parametric wall specimens focused in this study. As per the standards, the standard fire (ISO 834) temperature variation was considered on the fire exposed surface and the FRL is stated in terms of structural, integrity and insulation criteria. The structural FRL is the time in minutes that a building component can withstand the structural loads, at the exposure to a fire accident. Then the integrity failure is referred to the time in minutes that a fire exposed building component loses its integrity and becomes unable to avoid hot flames and gases passing through itself. Similarly, the insulation FRL has been stated as the time in minutes, that a fire exposed building component's unexposed surface temperature increasing beyond a threshold temperature. The standards declare, an average temperature increment by 140°C or a maximum temperature on the surface increment by 180°C as the limit for the insulation FRL. Since room temperature is assumed to be 20°C as per the industry practice, an average temperature rise of 160°C and a maximum temperature rise of 200°C have been considered as the insulation fire failure incident.

Initially, the Finite Element Models (FEMs) have been developed for the original and parametric wall specimens following successful validation of the FEM methods. The Heat Transfer Analyses (HTA) results produced subsequently have been used to derive the time to reach average and maximum temperature on the unexposed surfaces of the modular walls to 160°C and 200°C respectively. The lesser time is produced as the insulation FRL. Thereafter, structural fire resistance of the wall specimens could also be derived from the HTA results comparing against the relationship of LR versus critical steel temperature of the SHS steel column at the structural fire failure explained in the next sub-section.

2.2. Structural failure of SHS columns at elevated temperatures

At the elevated temperatures, reduction of mechanical strengths and the resulting lower loadbearing and structural performance degradation are always being critical for any structural component of steel material. As a steel column in compression is exposed to fire or elevated temperature, the compressive strength will be progressively reduced as steel temperature rises. The designing of structural members, allow a reasonable safety factor. Hence at the ambient temperature, the compressive stresses, built up in the steel section are maintained to be a factor from the compressive strength of steel material. However, as the structural element is subjected to elevated temperatures in case of a fire accident, the compressive strength continues to be reduced, and at a certain instance, the applied compressive stresses will be matched by the compressive strength and at the next instance applied stresses will overcome the material strength leading those elements on the column section to fail in compression. Thereafter, the column will start to experience asymmetric compression load and hence the compression stresses of some elements will be increased as well. Those increased stresses at certain elements will now surpass the compression strength at the section, making those elements to fail in compression as well. In this manner, the eccentricity of the asymmetric load will even increase resulting excessive buckling and ultimate structural failure of the steel column. Therefore, the structural failure of a steel column at an elevated temperature is governed by the applied compression load and the critical steel temperature. For instance, if the ratio of applied compressive stress to the compressive strength of steel at the ambient temperature is low, the steel member will need to reach a higher temperature to reduce the compressive strength of steel to

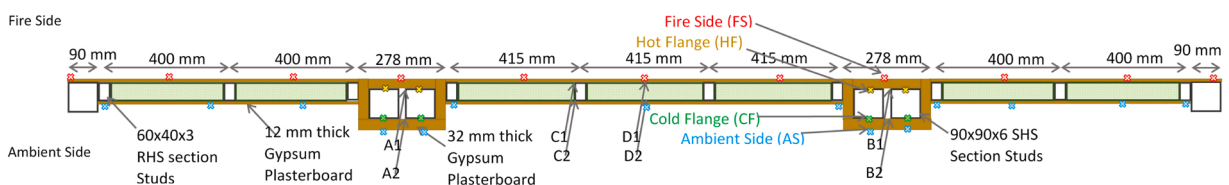


Fig. 2. Loadbearing modular wall panel from Yu et al. [20].

match the compressive stress applied. Again, if the compressive stresses are higher, at a lower temperature rise, the steel member will reach that compressive strength. Here the compressive stress is a function of applied load on the steel column while the compressive strength of steel material can be related to the load carrying capacity at the ambient temperature.

Hence, many researchers including Gunalan et al. [22], Chen et al. [23] Dias et al. [4], Balarupan [24] and Kesawan et al. [25] have addressed the Load Ratio (LR) which is defined as the ratio of applied load over the ambient temperature load carrying capacity to describe the elevated temperature structural failure of steel columns and studs. Among those research studies, Balarupan [24] has investigated on and SHS section steel columns against the axial compression capacity at elevated temperature addressing a range of parameters. In that study, SHS section width has been varied from 65 mm to 200 mm, section thickness from 3 mm to 16 mm and the length of the column from 1.5 m to 18 m. The elevated temperature compression failure of the parametric columns has been determined from experimental investigations followed by design calculations and FEM techniques. Those data have been extracted from the literature and the LR versus critical temperature of SHS columns at the structural failure has been plotted in Fig. 3.

The resulted relationship is a 5th order polynomial from which the critical steel temperature at the structural failure can be derived at the required LR value as presented in Table 1. Firstly, the time – temperature variations of the steel columns are to be produced from the FEM and HTA. Secondly, Fig. 3 can be referred to read the critical steel temperature related to the structural failure for the applied LR value. Afterwards the time-temperature variations of the SHS column have to be analysed against that critical steel temperature to determine the time for the structural failure. Although, the LR versus critical steel temperature at failure for the SHS section columns have been based on the behaviour of columns alone, the same correlation could be used for the analysis of modular wall panels in the current study, since it is only the SHS section columns act as the structural elements in the wall. More specifically, even the non-loadbearing studs and the wall panels could experience the integrity or insulation failure earlier, the SHS section columns would continue to support the structure until the columns reach the individual structural failure. However, slight deviations can be expected due to the modified restrain conditions. Still the structural failures predicted using the LR versus critical steel temperature serves as a robust technique of evaluating the structural FRL of the modular walls with a reasonable safety margin.

3. Numerical analyses

With the presence of reliable full-scale fire tests on the original wall panel, thermal properties of the incorporated material, and with the understanding on FE and HTA techniques, an extensive scale 2D and 3D numerical studies have been conducted to identify the influence of non-loadbearing stud choice, thickness of plasterboard sheathing on the loadbearing columns and the cavity Insulation Ratio (IR). For all the FEM studies, ABAQUS CAE, the commercially available software package [26] has been used, carefully choosing the reliable elevated temperature thermal properties of the used material and correct FE methods followed by the validation of numerical models against the relevant experimental data.

3.1. Thermal properties of wall specimen materials

It is well understood that the thermal properties, namely the thermal conductivity, specific heat and density govern any HTA and at a fire accident when the materials are subjected to elevated temperatures those thermal properties are highly affected. Hence, the use of reliable thermal properties is essential in order to produce realistic HTA results. The non-loadbearing studs have been changed from RHS steel section to LCS steel section and to rectangular solid timber section studs. The other material involved in the parametric wall panel designs are the gypsum plasterboard and mineral wool insulation material. However, validation of the thermal properties and

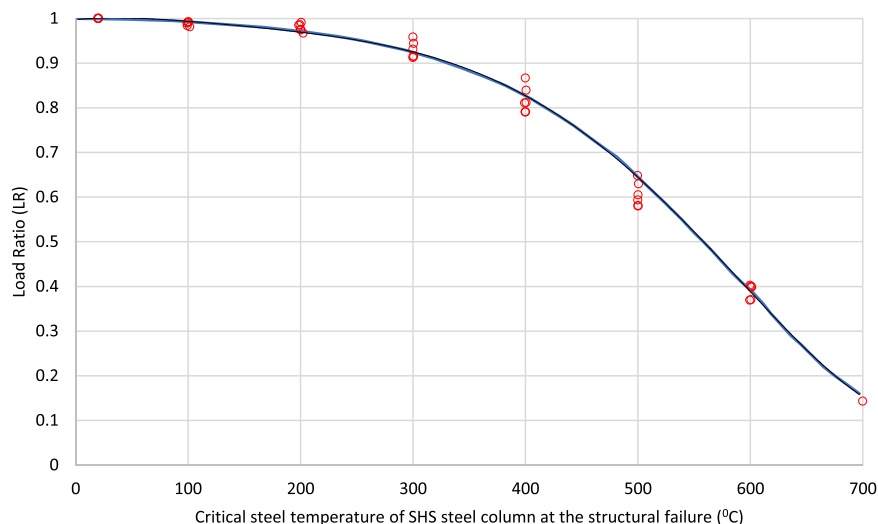


Fig. 3. LR versus critical steel temperature of SHS steel column at the structural failure; data extracted from Balarupan et al. [24].

Table 1

Critical steel temperature of SHS section columns at the structural failure for different LR values.

| LR | 0.2 | 0.3 | 0.4 | 0.5 | 0.6 | 0.7 | 0.8 |
|--|-------|-------|-------|-------|-------|-------|-------|
| Critical Steel Temperature (°C) | 659.3 | 648.8 | 631.4 | 607.0 | 557.0 | 492.3 | 386.3 |

FEM techniques is essential. In this instance, plywood, rockwool and glass-fibre material have also been used in those models developed for the validation purpose. Hence, the elevated temperature thermal properties of steel, timber, mineral wool, rockwool, glass-fibre, gypsum plasterboard and plywood have been adopted in FEA as presented in Table 2 along with the references those have been extracted from. The time variant behaviours of specific heat of steel and gypsum wall boards can be well understood against the change of phases and chemical reactions in the materials where the peaks of specific heat graphs in Table 2 are directly related to those incidents. Since the plasterboard cracking cannot be physically simulated in the HTA stage of the FEMs, elevated temperature thermal properties at higher temperatures have been modified as per the previous research evidence [14,27,28] on the FEM techniques of fire exposed walls and floors. However, such apparent thermal properties have proven to produce realistic time-temperature variations of fire exposed walls and floors at different thicknesses with respect to the experimental results.

3.2. FEM details

This section describes the FEM techniques used and the methods followed in developing the FEMs in ABAQUS CAE software, for simulating full-scale fire exposed tests of the modular wall panels under consideration. The main objectives of FEM analyses are to simulate the experimental conditions, conduct HTA and derive realistic time dependent temperature variations using numerical approaches. With the availability of accurate full-scale experimental data, the FEM techniques and thermal properties have been first successfully validated and then the same approaches have been confidently applied to produce results for the parametric modular walls.

The initial step in developing a FEM is to create all the parts involved in the wall design and to apply correct thermal properties and mesh details. If this is illustrated with the original wall panel, the 90 × 90 × 6 mm SHS columns of 3 m length, 60 × 40 × 3 mm RHS studs of 3 m length, all the insulation parts and plasterboard sheathing parts were developed. Thermal properties of gypsum, steel, and mineral wool were assigned to the model creating the related material types. The sections of plasterboard, SHS, RHS, insulation components were then modelled integrating the material type as per the design. Those sections were subsequently assigned to the created parts so that each part is modelled with the correct material properties.

Next, all parts were meshed, assigning structured hexahedron shaped, 8-node heat transfer brick elements (DC3D8 available in the ABAQUS CAE library). Linear interpolation was set for the geometric order and the standard heat transfer elements have been used where numerical integration was applied. The selection of mesh densities was carefully carried out followed by a mesh sensitivity analysis. Ultimately, the through thickness mesh density was set at 2 mm for each part while the global mesh is at 10 mm. Fig. 4 shows a picture of the developed FEM for the original modular wall panel indicating the finite mesh. The assignment of Heat Transfer (HT) brick finite elements will make sure the conduction mode heat transfer from one element to the next inside the same part is enabled. However, the conduction mode HT, from one part to the adjacent which are in contact, the convection mode HT on the fire exposed and unexposed surfaces, and the radiation mode HT of those surfaces must be separately modelled using constraints and interactions present in the software tools.

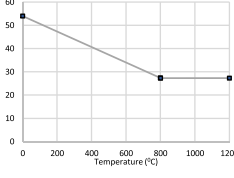
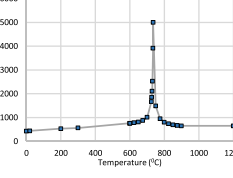
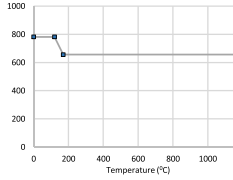
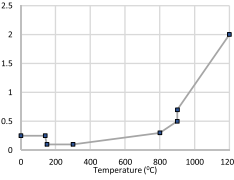
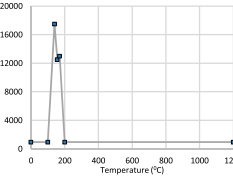
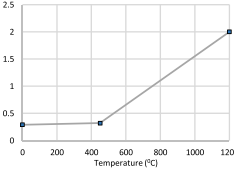
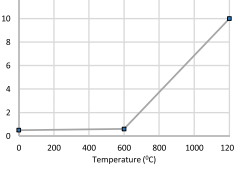
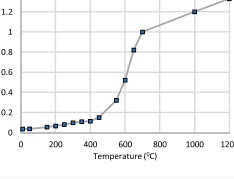
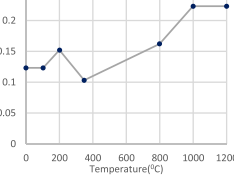
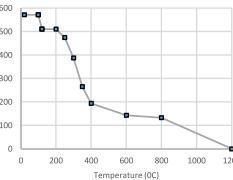
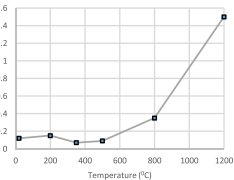
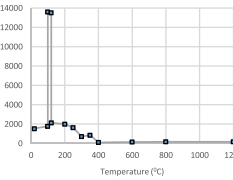
To apply the fire load on the modular wall, the standard fire temperatures (θ in °C) expressed in Eq. (1) were assigned to the fire exposed surface as a temperature boundary condition. Tie constraints were introduced between each adjacent parts in contact, enabling the conduction mode heat transfer as described earlier. Then the fire exposed surface and the unexposed side surface were assigned with convection and radiation mode interactions where the convection film coefficients were 25 W/(m °C) and 10 W/(m °C) respectively, and the radiation emissivity was set at 0.9. Besides this HT inside the cavity surfaces were also simulated defining closed cavity radiation interactions with 0.9 emissivity. It should be noted that the wall panel had been covered with two plasterboards on top and bottom, so that the cavity regions were in fact closed cavities and that related to the real application as well. Moreover, the airflow in the cavity regions is restricted and the convection mode HT can be reasonably neglected in the HTA. Also, when applying tie constraints for the perfect conduction mode heat transfer, any heat loss would be marginal since convection and radiation mode heat transfers and the apparent thermal properties have been adjusted in a way, that the FEM simulate realistic conditions.

$$\theta = 345 \log_{10}(8t + 1) + 20 \quad (1)$$

The boundary conditions and interactions defined on the FEM have been summarised and illustrated in Fig. 5.

Initially, the whole wall panel is in room temperature, and when the fire accident takes place the fire load boundary conditions and the relevant interactions need to be enabled. This scenario was obtained using the step procedure available in the library. The initial step and a following HT step were defined. The first increment of the HT step is set at 10 s and the automatic incrementation was enabled so that the ABAQUS software would determine each following step size analysing the convergence of the heat transfer results. Here the maximum number of increments and the minimum increment size were set to 100 million and 0.01 s respectively to ensure converged results without the analysis being terminated until the specified total time period (14,400 s). Then in the initial step, a predefined field of constant temperature was applied on every instance of the model. Thereafter, the temperature boundary conditions, and the connection and radiation interactions were applied using the HT step. That way, the initial conditions before fire and the

Table 2
Thermal properties of the materials involved in the numerical study [27,29–33].

| Material | Density (kg/m ³) | Thermal Conductivity (W/m.°C) | Specific Heat (J/kg.°C) |
|-----------------------|---|---|---|
| Steel [29] | 7850 |  |  |
| Gypsum Board [27] |  |  |  |
| Rock Wool [27] | 100 |  | 840 |
| Glass Fibre [27] | 15.42 |  | 900 |
| Mineral Wool [30, 31] | 80 |  | 840 |
| Plywood [32] | 500 |  | 1500 |
| Timber [33] |  |  |  |

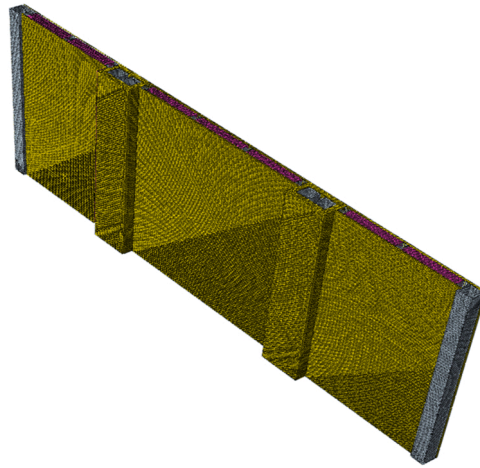


Fig. 4. FE model of the original modular wall with the finite mesh.

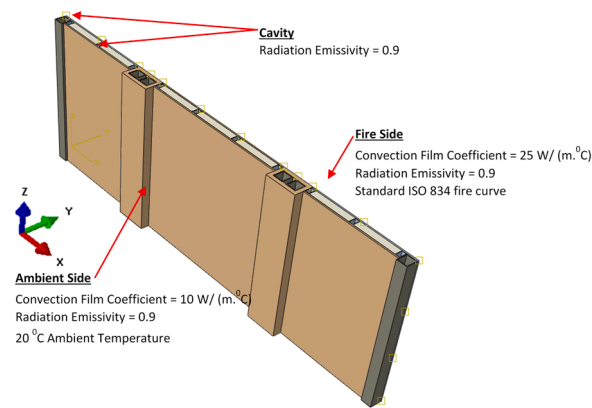


Fig. 5. Boundary conditions and interactions defined on the FEM.

conditions during the fire are realistically simulated in the FEA procedures. Finally, the HTA were run on the developed FEM, and the time – temperature variations at the required points of the model were obtained for 4 h fire exposure. The observed points had been chosen to produce the temperatures on Fire Side (FS), Hot-Flange (HF), Cold-Flange (CF) and Ambient Side or the unexposed side (AS). The term HF is referred to the flange of the SHS section column closer to the FS and the term CF to which is closer to the AS. When monitoring the AS temperature, the maximum and the average temperature readings were obtained.

3.3. Validation of FEMs

Despite of all previous studies and reliable sources of which the thermal properties and FEM techniques have been extracted from, accurate validation is the assurance of reliability of the current study. Hence the original wall frame experimented by Yu et al. [20], the Light Frame Timber (LFT) experimented by Kolaitis et al. [34] and the five LSF wall panels experimented by Gunalan et al. [22] have been numerically analysed with the ABAQUS CAE using the thermal properties presented in Section 3.1 and the FEM techniques explained in Section 3.2. The produced time variant temperature plots at the required points on the wall panels have been afterwards compared against the experimental temperature profiles as presented in Figs. 6–8.

The original wall frame in Fig. 6, consists of $90 \times 90 \times 6$ SHS section load bearing steel columns, $60 \times 40 \times 3$ non-loadbearing steel studs, 12 mm thick gypsum plasterboard wall boards, 32 mm thick gypsum plasterboards as column sheathing and mineral wool full cavity insulation. Then the LFT wall panel results shown in Fig. 7 consists of 12.5 mm thick Gypsum plasterboards, 10 mm thick plywood boards, 80×40 timber studs and rockwool full cavity insulation. Similarly, Fig. 8 presents the results of five LSF wall panels with $90 \times 40 \times 15 \times 1.15$ LCS steel studs, 16 mm gypsum plasterboards and with rockwool, mineral wool and glass fibre cavity insulation as indicated in the legend. The steel temperatures of A1, A2, B1 and B2 in Fig. 6 and HF and CF steel stud temperatures in Fig. 8 were especially studied for the accuracy of steel temperatures to which the structural fire failure had been correlated. Analysing all presented experimental versus FEM results, very good match between experimental and numerical approaches can be seen. Therefore, the accuracy of the thermal properties and the FEM details in the study were well validated and hence, the parametric

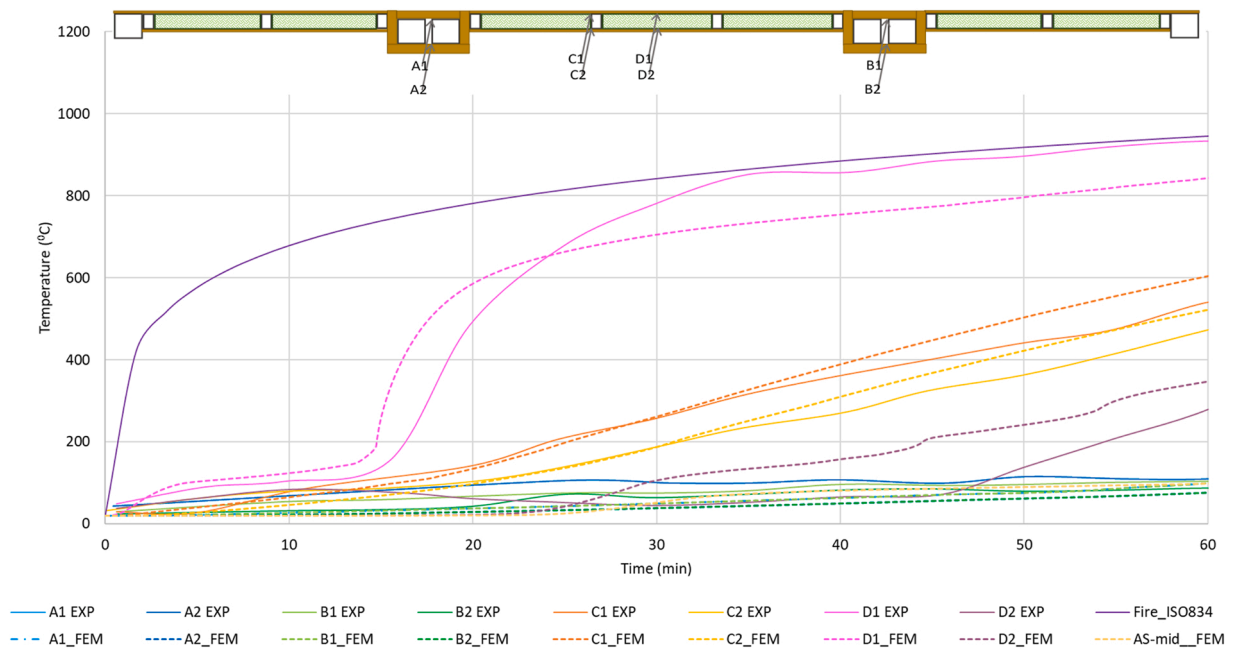


Fig. 6. Experimental [20] versus FEM temperature variations of the original wall frame of present study.

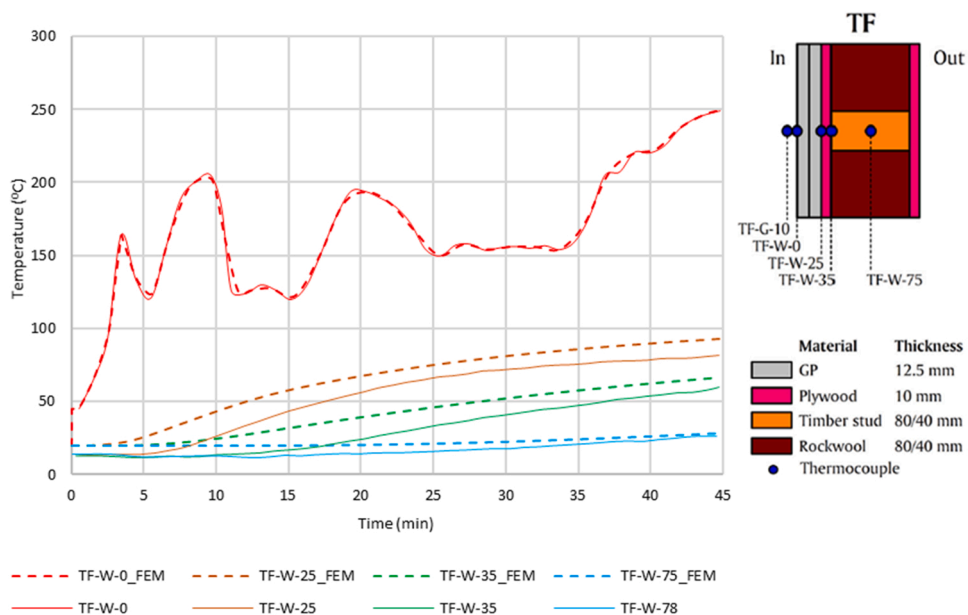


Fig. 7. Experimental [34] versus FEM temperature variations of LFT wall.

studies were confidently carried out applying the same thermal properties and FEM techniques and procedures.

The FEM analyses of the present study are limited to HTA where a different approach has been adopted for the evaluation of structural FRL monitoring the steel temperature variations derived from the same HTA results. Hence, only the validation of HTA methods have been presented in this section. However, the structural fire failures of different parametric SHS columns experimented and simulated by Balarupan et al. [24] had been used to produce the applied LR versus critical steel temperatures at the structural fire failure of SHS columns. In that study, heat transfer analysis of SHS columns had been first conducted followed by the coupled structural analyses introducing the appropriate mechanical properties of steel, loading conditions and boundary conditions. Geometrical imperfections had been proved to be negligible compared to the thermal bowing effect of the SHS columns at higher temperatures, and since sequential analyses techniques had been adopted, geometrical imperfection had not been counted. Ideally, fully coupled

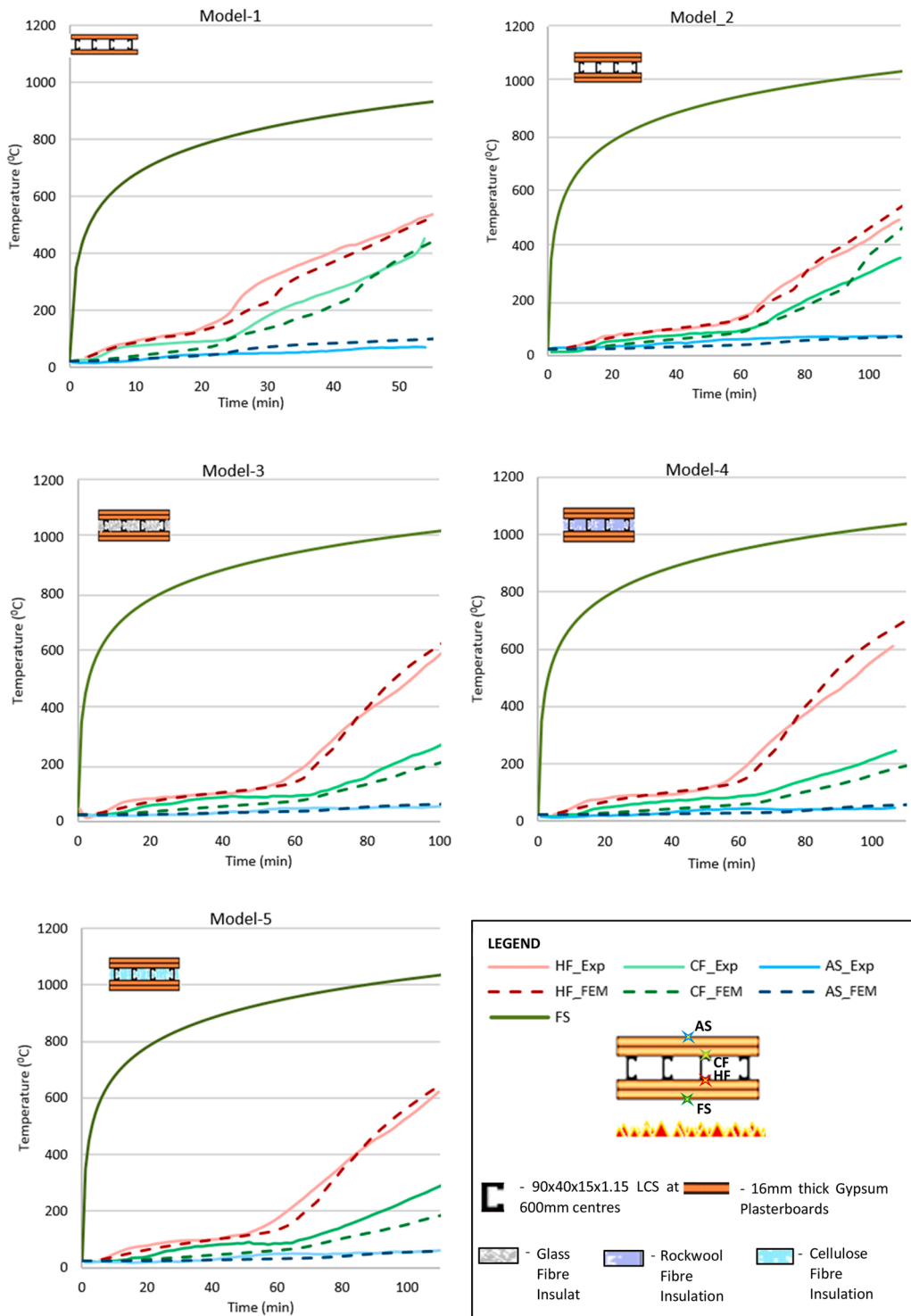


Fig. 8. Experimental [22] versus FEM temperature variations of five LSF wall panels.

thermal-mechanical analysis would simulate the exact experimental conditions of a structural fire test, where the SHS column is applied a constant load and subjected to the standard fire temperature curve until failure occurs. However, previous researchers [35] have proven that the sequentially coupled thermal-mechanical analyses provide quite realistic results at a huge saving of analysis time and computational power. With the availability of validation results presented in those previous studies [24], described structural fire analyses FEM techniques can be confidently applied in similar applications.

4. Parametric study and FEA results

The objective of this parametric study is to address the limitations of the original modular wall panel application related to material availability, construction efficiency and costs incurred. In this study, the loadbearing columns have been the $90 \times 90 \times 6$ SHS steel columns for all parameters, so that the ambient temperature structural performance of the wall specimens is the same. The non-loadbearing studs are $60 \times 40 \times 3$ RHS section steel studs in the original wall panel and this has been replaced with the $60 \times 40 \times 12 \times 1.5$ LCS CF steel stud and with the 60×40 softwood solid rectangular timber stud because LSF construction practice with CF studs and LFT with softwood timber studs are the most general practice in the European construction industry [36–38]. The design of original wall consists of 32 mm thick plasterboard sheathing on the loadbearing columns which is a quite expensive and heavier contribution to the wall panel although it provides admirable structural fire resistance by protecting the load bearers. However, it is worthwhile to investigate, if the insulation and integrity criterion based FRL of the wall panel reaches earlier, and then whether such thick layer of plasterboard necessary in this design. Also, the general practice in the construction industry is 9 mm, 12 mm, 16 mm thick plasterboards and to use double layer sheathing where necessary. Hence, in this study the variable of gypsum plasterboard thickness is set at 9 mm, 12 mm 16 mm and 32 mm. The other variable identified is the cavity IR. With respect to the LSF wall panel designs it has been found that the 0.2–0.4 IR will be more appropriate and efficient considering the structural and insulation FRL, energy efficiency requirements and the cost of the construction [18]. Therefore, it is necessary to conduct a similar parametric study in the current research scope. To summarise the parametric study plan, the non-loadbearing stud type, thickness of plasterboard sheathing around SHS section columns, and the cavity IR has been varied as shown in Fig. 9 with the applicable choices based on industry practice. FEM models were developed for parametric wall specimen and the HTA have been conducted. The resultant time-temperature variations were analysed to derive the FRLs. The temperature contours of two wall specimens with RHS studs, 32 mm column sheathing and cavity insulation at 0.6 IR and 1.0 IR have been presented in Fig. 10 and Fig. 11 respectively. The FRLs derived for each parametric wall panel have been presented in Table 3.

4.1. Structural Fire Resistance Level

Determination of the structural FRL is progressed as explained in Section 2. The LR versus critical steel temperature of SHS section at the structural failure relationship was referred to read the critical temperatures at 0.2–0.8 LR values. As explained in Section 2.2, when the HF temperature of the SHS column go beyond the threshold temperature obtained from that relationship, the structural failure of the SHS column takes place. Therefore, developing a FEM model for every parametric wall panel according to the FEM details presented in the previous section, HTA is conducted, and the time-temperature variations of FS, HF, CF and AS are obtained. The HF temperature versus time plot was then analysed against the critical temperatures obtained from LR versus critical steel temperature graph so that the time taken for the HF temperature to reach the critical temperature corresponding to the structural failure can be derived. In that way the structural FRL was determined for every parametric specimen over the LR values considered as presented in Fig. 12.

4.2. Insulation Fire Resistance Level

Temperature limits of 160 °C and 200 °C were identified as the average and maximum temperature thresholds on the unexposed or AS surface of the parametric walls in evaluating the insulation FRL. As explained in the previous section, average and maximum AS temperature variations were produced from the HTA conducted on the FEMs. Afterwards, the average AS temperature was compared against 160 °C and the maximum AS temperature against 200 °C. The earliest time of average temperature reaching 160 °C and maximum temperature reaching 200 °C has been provided as the insulation FRL. The insulation FRLs determined for the parametric study are graphed in Fig. 13.

4.3. Discussion

The trends of structural and insulation FRLs, determined from FEA studies have been analysed against each variable. The choice of non-loadbearing studs between RHS steel stud, LCS CF steel stud and the softwood solid rectangular stud prove to induce no significant influence either on structural FRL or the insulation FRL of the wall panels. Hence, the choice of non-loadbearing stud type over these types can be independent from the required insulation and structural FRL. However, it might have significant influence on the energy

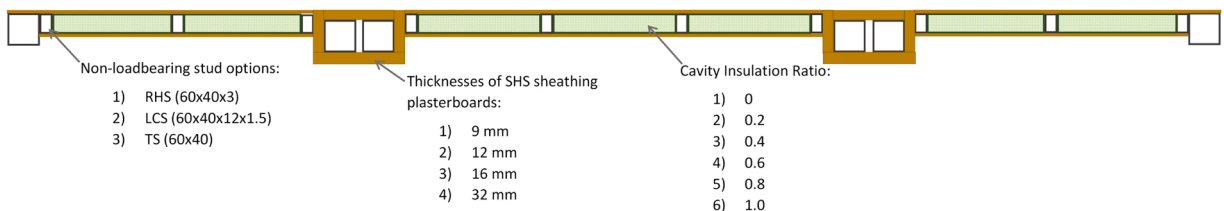


Fig. 9. Parametric study plan.

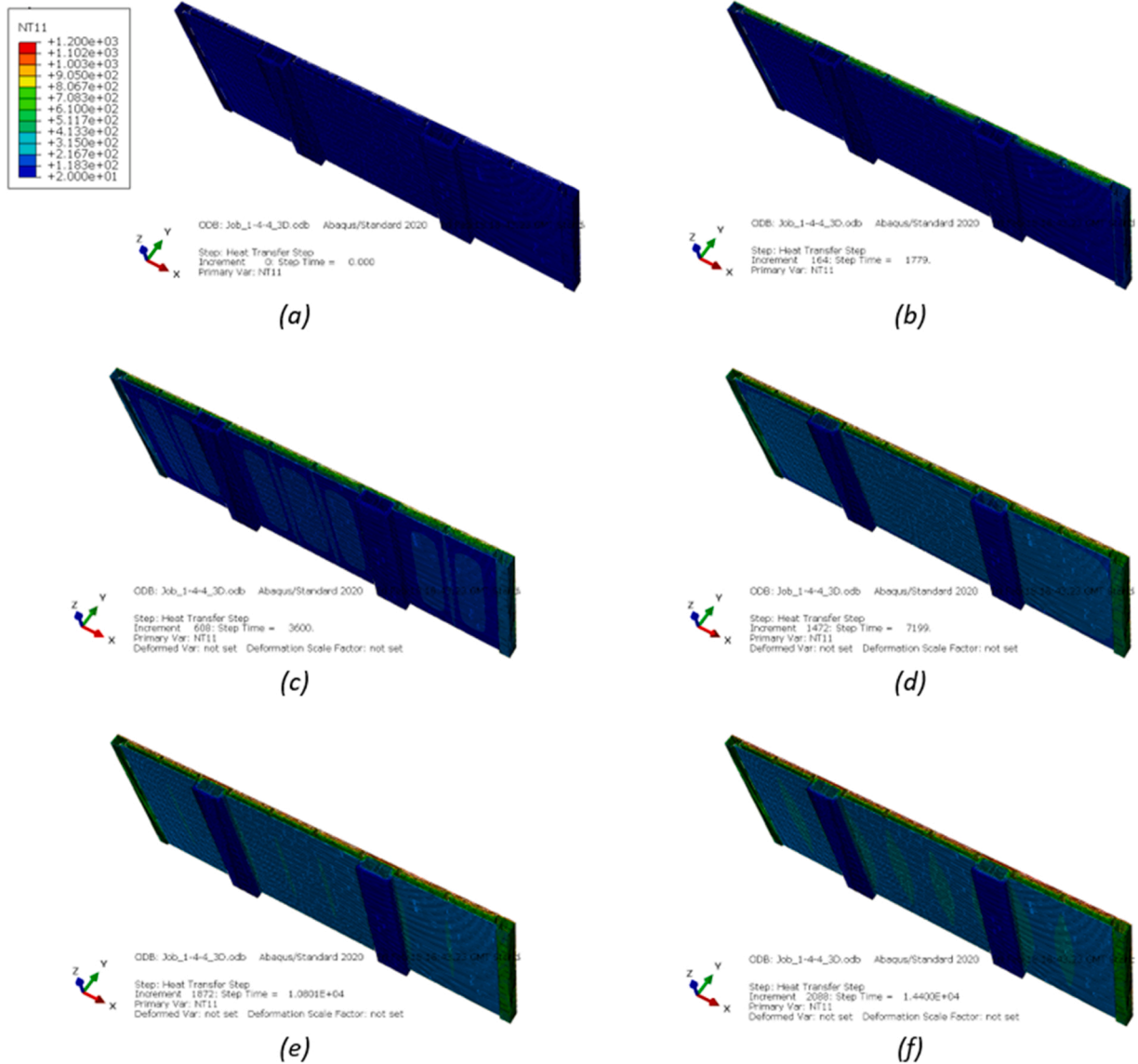


Fig. 10. HTA temperature contours of the wall specimen with RHS studs, 32 mm thick column sheathing and cavity insulation 0.6 IR at (a): 0 min; (b): 30 min; (c): 60 min; (d): 120 min; (e): 180 min & (f): 240 min.

efficiency, ease of manufacturing and the costs incurred.

Secondly, the plasterboard sheathing thickness around the SHS steel column has directly contributed to structural FRL while the influence on insulation FRL is negligible. The more the thickness of the plasterboard sheathing is, the lesser will be the HT to the HF from FS. Hence, the time for HF to reach a specific critical temperature corresponding to a LR value will be higher. The influence of plasterboard thickness on structural FRL can be explained with values related to 0.2 LR with 16 mm and 32 mm sheathing options. As the plasterboard thickness is doubled the structural FRL has been increased from 180 min to 210 min which means a 50% improvement. However, the plasterboard sheathing thickness of the wall panel remained at 12 mm for all the specimens and hence, the HT through the wall section has been the same for all cases resulting similar insulation FRLs over the plasterboard thickness around the SHS columns.

The remaining variable, the cavity IR has no noticeable influence over the structural FRL, however a significant influence on the insulation FRL. From non-insulated (0 IR) to full-cavity (1.0 IR) insulation options the insulation FRL has been linearly increased from 52 min to 86 min for all column plasterboard options and non-loadbearing options. The influence of IR on the structural FRL is unique for the current study. In a previous study on LSF wall panels with channel section CF studs, lower the IR, it had been higher the structural FRL [12]. In case of channel section CF are applied as the load bearers in the LSF wall panel, the cavities between the channel sections and the wall boards had been filled with cavity insulation at different ratios, where increase of cavity IR discouraged the HT

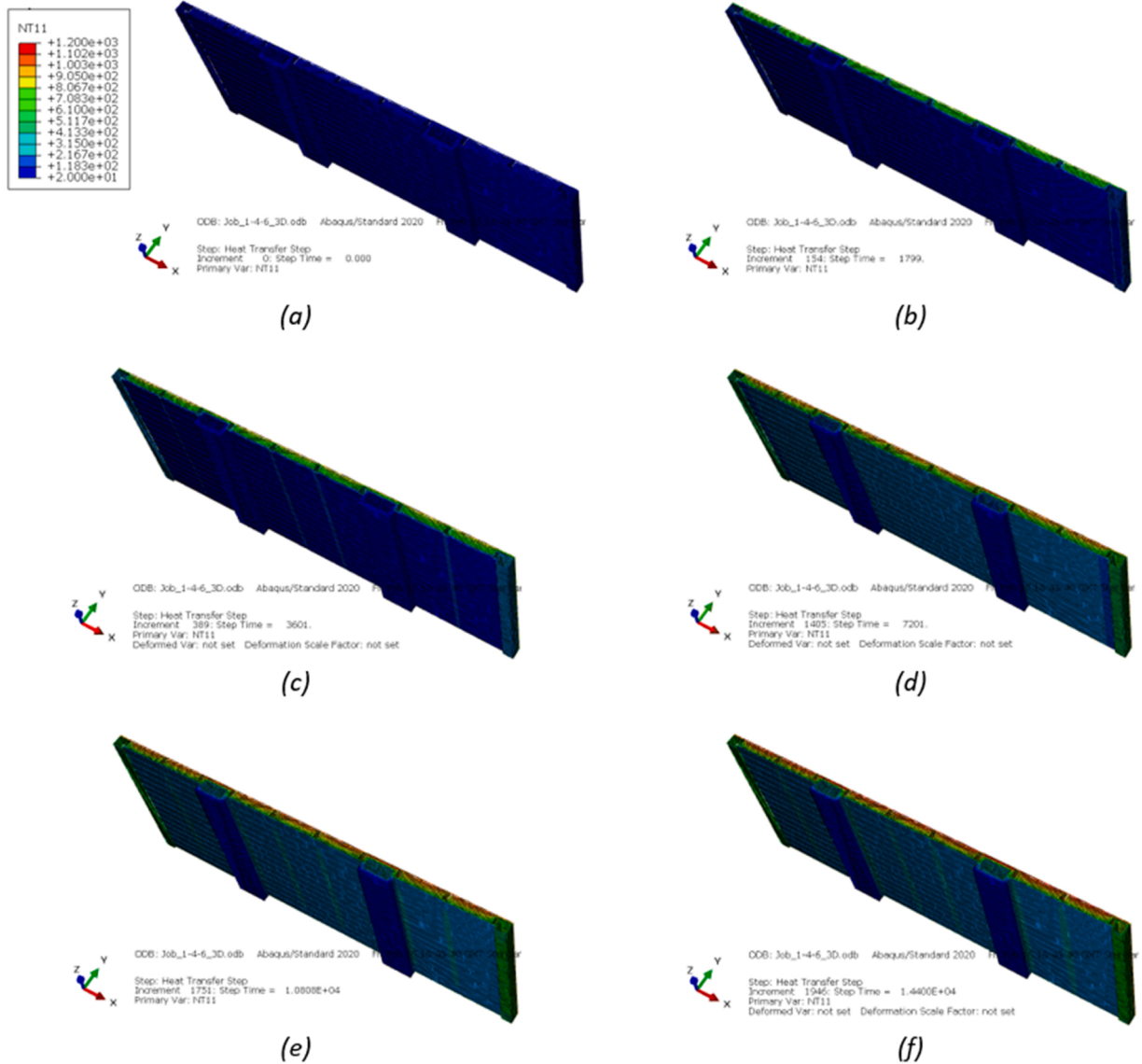


Fig. 11. HTA temperature contours of the wall specimen with RHS studs, 32 mm thick column sheathing and full cavity insulation at (a): 0 min; (b): 30 min; (c): 60 min; (d): 120 min; (e): 180 min & (f): 240 min.

from HF to the CF. Therefore, the heat transferred from the FS to HF had been accumulated resulting in increased HF temperatures and hence, reduced structural FRL. In contrary, the modular wall designs of the present study contain SHS steel studs thermally discontinued from the wall panel due to the plasterboard sheathing around them, so that the cavity insulation incorporated in the wall cavities (between non-loadbearing studs and the wall boards) has no influence over the structural FRL. Therefore, when choosing the appropriate cavity IR for this type of a modular wall, considerations toward the insulation FRL, energy performance requirements and cost terms would be sufficed while influence on structural FRL can be reasonably disregarded.

5. Summary

The research study presented in this paper is a detailed numerical analysis of a modular wall panel with loadbearing Square Hollow Section (SHS) steel columns. The objective of the investigation is to stretch the modular wall panel application limits, related to material availability, ease of manufacturing and construction procedures and costs assuring the insulation and structural FRLs. The loadbearing columns are separately sheathed with 32 mm thick gypsum plasterboard and the wall boards are of the same material but only 12 mm thick in the original wall panel. The cavities between non-loadbearing studs and the wall boards are fully insulated with mineral wool. The parametric study variables were chosen as the non-loadbearing stud type, thickness of plasterboard sheathing around the SHS columns and the cavity Insulation Ratio (IR).

Table 3
Fire ratings of parametric modular walls derived from HTA.

| Non-loadbearing stud type | Thickness of SHS sheathing (mm) | Insulation Ratio (IR) | FRL (min) against LR | | | | | | | | | | | | | | | |
|--|------------------------------------|-----------------------|----------------------|-------|-------|-------|-------|-------|-------|-------|-------|----|----|----|----|----|----|----|
| | | | 0.2 | 0.3 | 0.4 | 0.5 | 0.6 | 0.7 | 0.8 | | | | | | | | | |
| Rectangular Hollow Section (RHS) Studs | 9 | 0 | 41/-/ | 40/-/ | 38/-/ | 35/-/ | 30/-/ | 23/-/ | 14/-/ | 36 | 36 | 36 | 36 | 36 | 36 | 36 | 36 | |
| | | 0.2 | 44/-/ | 42/-/ | 36/-/ | 29/-/ | 20/-/ | 18/-/ | 16/-/ | 63 | 63 | 63 | 63 | 63 | 63 | 63 | 63 | |
| | | 0.4 | 31/-/ | 27/-/ | 24/-/ | 21/-/ | 19/-/ | 17/-/ | 16/-/ | 69 | 69 | 69 | 69 | 69 | 69 | 69 | 69 | |
| | | 0.6 | 25/-/ | 24/-/ | 22/-/ | 21/-/ | 19/-/ | 17/-/ | 16/-/ | 75 | 75 | 75 | 75 | 75 | 75 | 75 | 75 | |
| | | 0.8 | 24/-/ | 24/-/ | 22/-/ | 21/-/ | 19/-/ | 17/-/ | 16/-/ | 81 | 81 | 81 | 81 | 81 | 81 | 81 | 81 | |
| | | 1.0 | 24/-/ | 24/-/ | 22/-/ | 21/-/ | 19/-/ | 17/-/ | 16/-/ | 87 | 87 | 87 | 87 | 87 | 87 | 87 | 87 | |
| | | 12 | 0 | 52/-/ | 51/-/ | 49/-/ | 46/-/ | 40/-/ | 32/-/ | 21/-/ | 54 | 54 | 54 | 54 | 54 | 54 | 54 | 54 |
| | | | 0.2 | 44/-/ | 42/-/ | 36/-/ | 29/-/ | 20/-/ | 17/-/ | 16/-/ | 63 | 63 | 63 | 63 | 63 | 63 | 63 | 63 |
| | | | 0.4 | 30/-/ | 28/-/ | 24/-/ | 21/-/ | 19/-/ | 17/-/ | 16/-/ | 69 | 69 | 69 | 69 | 69 | 69 | 69 | 69 |
| | | | 0.6 | 25/-/ | 24/-/ | 22/-/ | 21/-/ | 19/-/ | 17/-/ | 16/-/ | 75 | 75 | 75 | 75 | 75 | 75 | 75 | 75 |
| | 0.8 | | 24/-/ | 23/-/ | 22/-/ | 21/-/ | 19/-/ | 17/-/ | 16/-/ | 81 | 81 | 81 | 81 | 81 | 81 | 81 | 81 | |
| | 1.0 | | 24/-/ | 23/-/ | 22/-/ | 21/-/ | 19/-/ | 17/-/ | 16/-/ | 87 | 87 | 87 | 87 | 87 | 87 | 87 | 87 | |
| | 16 | | 0 | 52/-/ | 51/-/ | 49/-/ | 46/-/ | 40/-/ | 32/-/ | 21/-/ | 54 | 54 | 54 | 54 | 54 | 54 | 54 | 54 |
| | | | 0.2 | 44/-/ | 42/-/ | 36/-/ | 29/-/ | 20/-/ | 18/-/ | 16/-/ | 63 | 63 | 63 | 63 | 63 | 63 | 63 | 63 |
| | | | 0.4 | 30/-/ | 27/-/ | 24/-/ | 21/-/ | 19/-/ | 17/-/ | 15/-/ | 69 | 69 | 69 | 69 | 69 | 69 | 69 | 69 |
| | | | 0.6 | 25/-/ | 24/-/ | 22/-/ | 21/-/ | 19/-/ | 17/-/ | 16/-/ | 75 | 75 | 75 | 75 | 75 | 75 | 75 | 75 |
| | | 0.8 | 24/-/ | 23/-/ | 22/-/ | 21/-/ | 19/-/ | 17/-/ | 16/-/ | 81 | 81 | 81 | 81 | 81 | 81 | 81 | 81 | |
| | | 1.0 | 24/-/ | 23/-/ | 22/-/ | 21/-/ | 19/-/ | 17/-/ | 16/-/ | 87 | 87 | 87 | 87 | 87 | 87 | 87 | 87 | |
| | | 32 | 0 | 52/-/ | 51/-/ | 49/-/ | 46/-/ | 40/-/ | 32/-/ | 21/-/ | 54 | 54 | 54 | 54 | 54 | 54 | 54 | 54 |
| | | | 0.2 | 44/-/ | 42/-/ | 36/-/ | 29/-/ | 20/-/ | 18/-/ | 16/-/ | 63 | 63 | 63 | 63 | 63 | 63 | 63 | 63 |
| | | | 0.4 | 31/-/ | 28/-/ | 24/-/ | 21/-/ | 19/-/ | 17/-/ | 16/-/ | 69 | 69 | 69 | 69 | 69 | 69 | 69 | 69 |
| | | | 0.6 | 25/-/ | 24/-/ | 22/-/ | 21/-/ | 19/-/ | 17/-/ | 16/-/ | 75 | 75 | 75 | 75 | 75 | 75 | 75 | 75 |
| | 0.8 | | 25/-/ | 24/-/ | 22/-/ | 21/-/ | 19/-/ | 17/-/ | 16/-/ | 81 | 81 | 81 | 81 | 81 | 81 | 81 | 81 | |
| | 1.0 | | 25/-/ | 24/-/ | 22/-/ | 21/-/ | 19/-/ | 17/-/ | 16/-/ | 87 | 87 | 87 | 87 | 87 | 87 | 87 | 87 | |
| | Lipped Channel Section (LCS) Studs | | 9 | 0 | 50/-/ | 48/-/ | 46/-/ | 43/-/ | 37/-/ | 30/-/ | 21/-/ | 52 | 52 | 52 | 52 | 52 | 52 | 52 |
| | | | | 0.2 | 43/-/ | 41/-/ | 36/-/ | 29/-/ | 20/-/ | 18/-/ | 16/-/ | 61 | 61 | 61 | 61 | 61 | 61 | 61 |
| | | | | 0.4 | 31/-/ | 28/-/ | 24/-/ | 21/-/ | 19/-/ | 17/-/ | 16/-/ | 68 | 68 | 68 | 68 | 68 | 68 | 68 |
| | | | | 0.6 | 25/-/ | 24/-/ | 23/-/ | 21/-/ | 19/-/ | 17/-/ | 16/-/ | 75 | 75 | 75 | 75 | 75 | 75 | 75 |
| | | 0.8 | | 24/-/ | 24/-/ | 22/-/ | 21/-/ | 19/-/ | 17/-/ | 16/-/ | 81 | 81 | 81 | 81 | 81 | 81 | 81 | |
| | | 12 | 0 | 50/-/ | 48/-/ | 47/-/ | 43/-/ | 37/-/ | 30/-/ | 21/-/ | 52 | 52 | 52 | 52 | 52 | 52 | 52 | |
| 0.2 | | | 43/-/ | 41/-/ | 36/-/ | 29/-/ | 20/-/ | 18/-/ | 16/-/ | 61 | 61 | 61 | 61 | 61 | 61 | 61 | | |
| 0.4 | | | 31/-/ | 27/-/ | 24/-/ | 21/-/ | 19/-/ | 17/-/ | 16/-/ | 68 | 68 | 68 | 68 | 68 | 68 | 68 | | |
| 0.6 | | | 25/-/ | 24/-/ | 22/-/ | 21/-/ | 19/-/ | 17/-/ | 16/-/ | 75 | 75 | 75 | 75 | 75 | 75 | 75 | | |
| 0.8 | | | 24/-/ | 23/-/ | 22/-/ | 21/-/ | 19/-/ | 17/-/ | 16/-/ | 81 | 81 | 81 | 81 | 81 | 81 | 81 | | |

(continued on next page)

Table 3 (continued)

| Non-loadbearing stud type | Thickness of SHS sheathing (mm) | Insulation Ratio (IR) | FRL (min) against LR | | | | | | |
|-------------------------------------|---------------------------------|-----------------------|----------------------|-------|-------|-------|-------|-------|-------|
| | | | 0.2 | 0.3 | 0.4 | 0.5 | 0.6 | 0.7 | 0.8 |
| Solid Rectangular Timber Studs (TS) | 16 | 0.8 | 25/-/ | 24/-/ | 22/-/ | 21/-/ | 19/-/ | 17/-/ | 16/-/ |
| | | | 74 | 74 | 74 | 74 | 74 | 74 | 74 |
| | | 1.0 | 24/-/ | 23/-/ | 22/-/ | 21/-/ | 19/-/ | 17/-/ | 16/-/ |
| | | | 81 | 81 | 81 | 81 | 81 | 81 | 81 |
| | | 0 | 24/-/ | 24/-/ | 22/-/ | 21/-/ | 19/-/ | 17/-/ | 16/-/ |
| | | | 87 | 87 | 87 | 87 | 87 | 87 | 87 |
| | | 0.2 | 50/-/ | 49/-/ | 47/-/ | 43/-/ | 37/-/ | 30/-/ | 21/-/ |
| | | | 52 | 52 | 52 | 52 | 52 | 52 | 52 |
| | | 0.4 | 43/-/ | 41/-/ | 36/-/ | 29/-/ | 20/-/ | 18/-/ | 16/-/ |
| | | | 61 | 61 | 61 | 61 | 61 | 61 | 61 |
| | | 0.6 | 31/-/ | 28/-/ | 24/-/ | 21/-/ | 19/-/ | 17/-/ | 16/-/ |
| | | | 68 | 68 | 68 | 68 | 68 | 68 | 68 |
| | 0.8 | 25/-/ | 24/-/ | 22/-/ | 21/-/ | 19/-/ | 17/-/ | 16/-/ | |
| | | 74 | 74 | 74 | 74 | 74 | 74 | 74 | |
| | 1.0 | 25/-/ | 24/-/ | 22/-/ | 21/-/ | 19/-/ | 17/-/ | 16/-/ | |
| | | 81 | 81 | 81 | 81 | 81 | 81 | 81 | |
| | 32 | 0 | 24/-/ | 24/-/ | 22/-/ | 21/-/ | 19/-/ | 17/-/ | 16/-/ |
| | | | 87 | 87 | 87 | 87 | 87 | 87 | 87 |
| | | 0.2 | 50/-/ | 49/-/ | 46/-/ | 43/-/ | 37/-/ | 30/-/ | 21/-/ |
| | | | 52 | 52 | 52 | 52 | 52 | 52 | 52 |
| | | 0.4 | 43/-/ | 41/-/ | 36/-/ | 29/-/ | 20/-/ | 17/-/ | 16/-/ |
| | | | 61 | 61 | 61 | 61 | 61 | 61 | 61 |
| | | 0.6 | 31/-/ | 28/-/ | 24/-/ | 21/-/ | 19/-/ | 17/-/ | 16/-/ |
| | | | 68 | 68 | 68 | 68 | 68 | 68 | 68 |
| 0.8 | | 25/-/ | 24/-/ | 22/-/ | 21/-/ | 19/-/ | 17/-/ | 16/-/ | |
| | | 74 | 74 | 74 | 74 | 74 | 74 | 74 | |
| 1.0 | | 24/-/ | 24/-/ | 22/-/ | 21/-/ | 19/-/ | 17/-/ | 16/-/ | |
| | | 81 | 81 | 81 | 81 | 81 | 81 | 81 | |
| 9 | 0 | 24/-/ | 24/-/ | 22/-/ | 21/-/ | 19/-/ | 17/-/ | 16/-/ | |
| | | 87 | 87 | 87 | 87 | 87 | 87 | 87 | |
| | 0.2 | 50/-/ | 48/-/ | 46/-/ | 43/-/ | 38/-/ | 31/-/ | 21/-/ | |
| | | 52 | 52 | 52 | 52 | 52 | 52 | 52 | |
| | 0.4 | 44/-/ | 42/-/ | 36/-/ | 29/-/ | 20/-/ | 18/-/ | 16/-/ | |
| | | 62 | 62 | 62 | 62 | 62 | 62 | 62 | |
| | 0.6 | 31/-/ | 28/-/ | 24/-/ | 21/-/ | 19/-/ | 18/-/ | 16/-/ | |
| | | 69 | 69 | 69 | 69 | 69 | 69 | 69 | |
| | 0.8 | 25/-/ | 24/-/ | 22/-/ | 21/-/ | 19/-/ | 17/-/ | 16/-/ | |
| | | 76 | 76 | 76 | 76 | 76 | 76 | 76 | |
| | 1.0 | 25/-/ | 24/-/ | 22/-/ | 21/-/ | 19/-/ | 18/-/ | 16/-/ | |
| | | 82 | 82 | 82 | 82 | 82 | 82 | 82 | |
| 12 | 0 | 25/-/ | 24/-/ | 22/-/ | 21/-/ | 19/-/ | 18/-/ | 16/-/ | |
| | | 87 | 87 | 87 | 87 | 87 | 87 | 87 | |
| | 0.2 | 50/-/ | 48/-/ | 46/-/ | 43/-/ | 38/-/ | 31/-/ | 21/-/ | |
| | | 52 | 52 | 52 | 52 | 52 | 52 | 52 | |
| | 0.4 | 44/-/ | 42/-/ | 36/-/ | 29/-/ | 20/-/ | 18/-/ | 16/-/ | |
| | | 62 | 62 | 62 | 62 | 62 | 62 | 62 | |
| | 0.6 | 31/-/ | 28/-/ | 24/-/ | 21/-/ | 19/-/ | 17/-/ | 16/-/ | |
| | | 69 | 69 | 69 | 69 | 69 | 69 | 69 | |
| | 0.8 | 25/-/ | 24/-/ | 22/-/ | 21/-/ | 19/-/ | 17/-/ | 16/-/ | |
| | | 76 | 76 | 76 | 76 | 76 | 76 | 76 | |
| | 1.0 | 25/-/ | 24/-/ | 22/-/ | 21/-/ | 19/-/ | 18/-/ | 16/-/ | |
| | | 82 | 82 | 82 | 82 | 82 | 82 | 82 | |
| 16 | 0 | 25/-/ | 24/-/ | 22/-/ | 21/-/ | 19/-/ | 18/-/ | 16/-/ | |
| | | 87 | 87 | 87 | 87 | 87 | 87 | 87 | |
| | 0.2 | 50/-/ | 48/-/ | 46/-/ | 43/-/ | 38/-/ | 31/-/ | 21/-/ | |
| | | 52 | 52 | 52 | 52 | 52 | 52 | 52 | |
| | 0.4 | 44/-/ | 42/-/ | 36/-/ | 29/-/ | 20/-/ | 18/-/ | 16/-/ | |
| | | 62 | 62 | 62 | 62 | 62 | 62 | 62 | |
| | 0.6 | 31/-/ | 28/-/ | 24/-/ | 21/-/ | 19/-/ | 17/-/ | 16/-/ | |
| | | 69 | 69 | 69 | 69 | 69 | 69 | 69 | |
| | 0.8 | 25/-/ | 24/-/ | 22/-/ | 21/-/ | 19/-/ | 17/-/ | 16/-/ | |
| | | 76 | 76 | 76 | 76 | 76 | 76 | 76 | |
| | 1.0 | 24/-/ | 23/-/ | 22/-/ | 21/-/ | 19/-/ | 17/-/ | 16/-/ | |
| | | 82 | 82 | 82 | 82 | 82 | 82 | 82 | |
| 32 | 0 | 25/-/ | 24/-/ | 22/-/ | 21/-/ | 19/-/ | 17/-/ | 16/-/ | |
| | | 87 | 87 | 87 | 87 | 87 | 87 | 87 | |
| 0 | 49/-/ | 48/-/ | 46/-/ | 43/-/ | 38/-/ | 31/-/ | 21/-/ | | |
| | 52 | 52 | 52 | 52 | 52 | 52 | 52 | | |

(continued on next page)

Table 3 (continued)

| Non-loadbearing stud type | Thickness of SHS sheathing (mm) | Insulation Ratio (IR) | FRL (min) against LR | | | | | | | |
|---------------------------|---------------------------------|-----------------------|----------------------|-------|-------|-------|-------|-------|-------|--|
| | | | 0.2 | 0.3 | 0.4 | 0.5 | 0.6 | 0.7 | 0.8 | |
| | | 0.2 | 44/-/ | 42/-/ | 36/-/ | 29/-/ | 20/-/ | 18/-/ | 16/-/ | |
| | | 0.4 | 62 | 62 | 62 | 62 | 62 | 62 | 62 | |
| | | 0.6 | 69 | 69 | 69 | 69 | 69 | 69 | 69 | |
| | | 0.8 | 76 | 76 | 76 | 76 | 76 | 76 | 76 | |
| | | 1.0 | 82 | 82 | 82 | 82 | 82 | 82 | 82 | |
| | | | 24/-/ | 24/-/ | 22/-/ | 21/-/ | 19/-/ | 17/-/ | 16/-/ | |
| | | | 87 | 87 | 87 | 87 | 87 | 87 | 87 | |

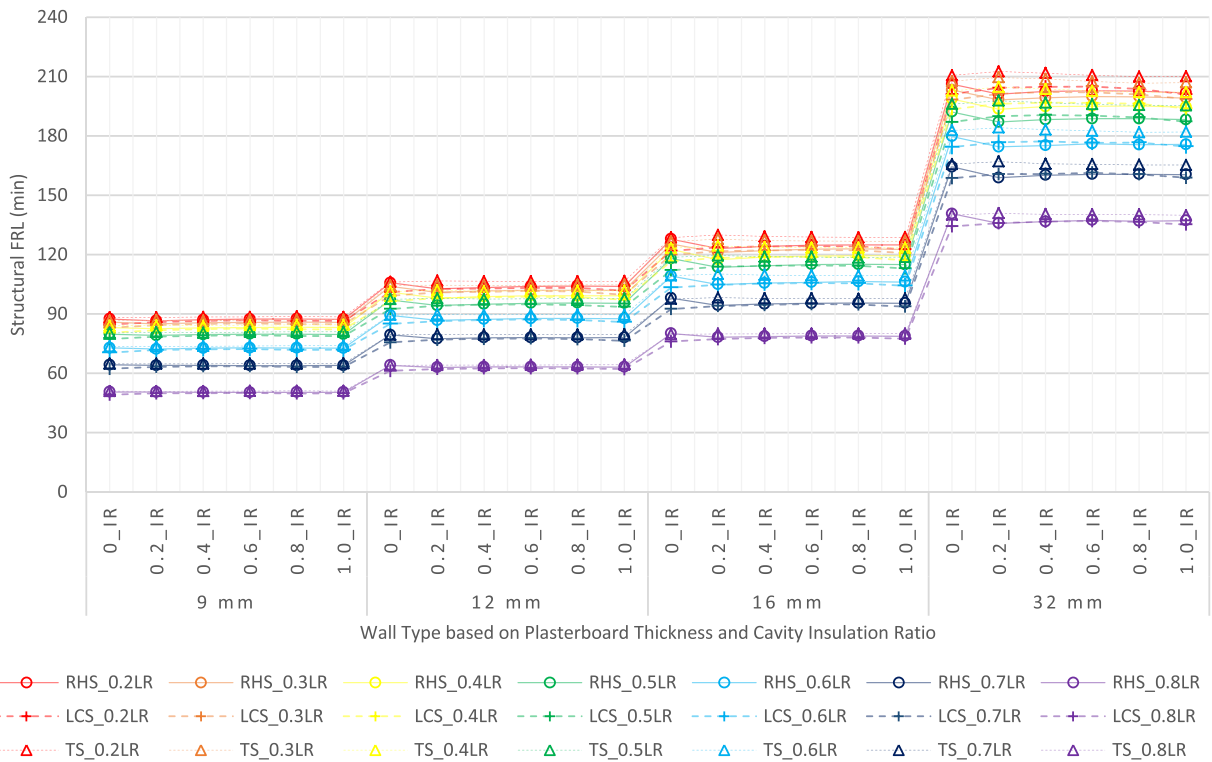


Fig. 12. Structural FRL of parameters against LR.

Seven full scale fire experiments have been simulated with Finite Element Models (FEM) developed with ABAQUS CAE software. The validation results of those experimental versus numerical data have proven the accuracy of the thermal properties and the FEM methods followed. Hence, the same numerical approaches had been confidently applied to the parametric study to produce Fire Side (FS), Hot-Flange (HF), Cold-Flange (CF) and Ambient Side (AS) temperatures. Simultaneously, a previous experimental and Finite Element (FE) study on the elevated temperature structural failure of SHS section columns was referred to produce a correlation between the Load Ratio (LR) and the critical steel temperature of the SHS section column at the structural failure. That relationship along with the HF temperature plots derived from FE study for each parameter was used to evaluate the structural FRL at different LRs. Furthermore, AS temperature plot was analysed against 140 °C and 180 °C, average and maximum temperature rise thresholds to find the insulation FRL.

The conclusions have been obtained with respect to each variable concerned. The non-load bearing stud type was changed from Rectangular Hollow Section (RHS) steel stud to Lipped Channel Section (LCS) CF steel stud and to softwood solid rectangular timber stud, where no effective influence was seen against the structural or insulation FRL. Then the SHS sheathing thickness has proven to make a significant effect on the structural FRL however, no influence made against the insulation FRL. Meanwhile, the cavity IR has been linearly influenced the insulation FRL, but not on the structural FRL.

In conclusion the modular wall panel investigated in the study claims several design guidelines considering the structural and insulation FRL. The selection of non-loadbearing stud section is released from the effect on structural or insulation FRL, so that energy

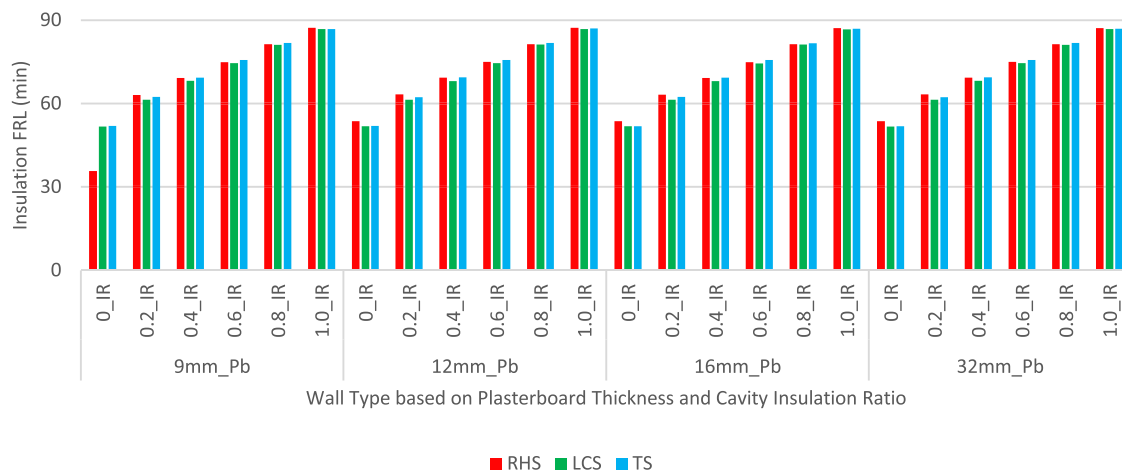


Fig. 13. Insulation FRL for parameters.

efficiency, cost and convenience of manufacturing may govern. The thickness of SHS column sheathing can be selected considering the required structural FRL and no attention is required on the insulation FRL. However, cost, energy and influence on the manufacturing and construction stages may need consideration. Finally, the IR should be chosen with respect to the insulation FRL requirement while structural FRL is disregarded. Again, the limitations and standards on energy performance, costs and construction and manufacturing procedures will have a significant control over this variable. Therefore, as a recommendation, a comprehensive investigation on the energy performance, cost terms and limitations related to manufacturing and construction phases of this modular wall is very necessary and further study is underway.

Declaration of Competing Interest

The authors declare that they have no known competing financial interests or personal relationships that could have appeared to influence the work reported in this paper.

Acknowledgements

The authors would like to acknowledge the ESS Modular Limited and Northumbria University for the financial support and research facilities.

References

- [1] J.Y.R. Liew, Y.S. Chua, Z. Dai, Steel concrete composite systems for modular construction of high-rise buildings, *Structures* 21 (2019) 135–149, <https://doi.org/10.1016/j.istruc.2019.02.010>.
- [2] Y. Dias, P. Keerthan, M. Mahendran, Predicting the fire performance of LSF walls made of web stiffened channel sections, *Eng. Struct.* 168 (2018) 320–332, <https://doi.org/10.1016/j.engstruct.2018.04.072>.
- [3] Y. Dias, M. Mahendran, K. Poologanathan, Full-scale fire resistance tests of steel and plasterboard sheathed web-stiffened stud walls, *Thin-Walled Struct.* 137 (2019) 81–93, <https://doi.org/10.1016/j.tws.2018.12.027>.
- [4] Y. Dias, M. Mahendran, K. Poologanathan, Axial compression strength of gypsum plasterboard and steel sheathed web-stiffened stud walls, *Thin-Walled Struct.*, vol. 134, pp. 203–19, 2019. (<https://doi.org/10.1016/j.tws.2018.10.013>).
- [5] S. Gunalan, M. Mahendran, Fire performance of cold-formed steel wall panels and prediction of their fire resistance rating, *Fire Saf. J.* 64 (2014) 61–80, <https://doi.org/10.1016/j.firesaf.2013.12.003>.
- [6] P. Keerthan, M. Mahendran, Thermal performance of composite panels under fire conditions using numerical studies: plasterboards, rockwool, glass fibre and cellulose insulations, *Fire Technol.* 49 (2) (2013) 329–356, <https://doi.org/10.1007/s10694-012-0269-6>.
- [7] D. Perera, et al., Fire performance of modular wall panels: Numerical analysis, *Structures* 34 (2021) 1048–1067, <https://doi.org/10.1016/j.istruc.2021.06.111>.
- [8] D. Perera, et al., Fire performance of cold, warm and hybrid LSF wall panels using numerical studies, *Thin-Walled Struct.* 157 (2020), 107109, <https://doi.org/10.1016/j.tws.2020.107109>.
- [9] Y. Dias, P. Keerthan, M. Mahendran, Fire performance of steel and plasterboard sheathed non-load bearing LSF walls, *Fire Saf. J.* 103 (2019) 1–18, <https://doi.org/10.1016/j.firesaf.2018.11.005>.
- [10] M. Rusthi, A. Ariyanayagam, M. Mahendran, P. Keerthan, Fire tests of magnesium oxide board lined light gauge steel frame wall systems, *Fire Saf. J.* 90 (2017) 15–27, <https://doi.org/10.1016/j.firesaf.2017.03.004>.
- [11] R. Lawson, A. Way, M. Heywood, J. Lim, R. Johnston, K. Roy, Stability of light steel walls in compression with plasterboards on one or both sides, *Proc. Inst. Civ. Eng. - Struct. Build.* 173 (2019) 1–61, <https://doi.org/10.1680/jstbu.18.00118>.
- [12] D. Perera, et al., Novel conventional and modular LSF wall panels with improved fire performance, *J. Build. Eng.* (2021), 103612, <https://doi.org/10.1016/j.jobte.2021.103612>.
- [13] K. Roy, et al., Collapse behaviour of a fire engineering designed single-storey cold-formed steel building in severe fires, *Thin-Walled Struct.* 142 (2019) 340–357, <https://doi.org/10.1016/j.tws.2019.04.046>.
- [14] P. Gatheeshgar, et al., On the fire behaviour of modular floors designed with optimised cold-formed steel joists, *Structures* 30 (2021) 1071–1085, <https://doi.org/10.1016/j.istruc.2021.01.055>.

- [15] E. Rodrigues, N. Soares, M.S. Fernandes, A.R. Gaspar, Á. Gomes, J.J. Costa, An integrated energy performance-driven generative design methodology to foster modular lightweight steel framed dwellings in hot climates, *Energy Sustain. Dev.* 44 (2018) 21–36, <https://doi.org/10.1016/j.esd.2018.02.006>.
- [16] E. Roque, P. Santos, The effectiveness of thermal insulation in lightweight steel-framed walls with respect to its position, *Spec. Issue Insul. Mater. Resid. Build.* 7 (1) (2017) 18, <https://doi.org/10.3390/buildings7010013>.
- [17] E. Roque, R. Vicente, R.M.S.F. Almeida, Opportunities of light steel framing towards thermal comfort in southern European climates: long-term monitoring and comparison with the heavyweight construction, *Build. Environ.* 200 (2021), 107937, <https://doi.org/10.1016/j.buildenv.2021.107937>.
- [18] D. Perera, et al., Energy performance of fire rated LSF walls under UK climate conditions, *J. Build. Eng.* 44 (2021), 103293, <https://doi.org/10.1016/j.jobe.2021.103293>.
- [19] R.M. Lawson, Light steel modular construction, in: Technical Information Sheet ED014, The Steel Construction Institute, 2012.
- [20] Y. Yu, P. Tian, M. Man, Z. Chen, L. Jiang, B. Wei, Experimental and numerical studies on the fire-resistance behaviors of critical walls and columns in modular steel buildings, *J. Build. Eng.* 44 (2021), 102964, <https://doi.org/10.1016/j.jobe.2021.102964>.
- [21] M. Bellová, EUROCODES: structural fire design, *Procedia Eng.* 65 (2013) 382–386, <https://doi.org/10.1016/j.proeng.2013.09.059>.
- [22] S. Gunalan, P. Kolarikar, M. Mahendran, Experimental study of load bearing cold-formed steel wall systems under fire conditions, *Thin-Walled Struct.* 65 (2013) 72–92, <https://doi.org/10.1016/j.tws.2013.01.005>.
- [23] W. Chen, J. Ye, Y. Bai, X.-L. Zhao, Improved fire resistant performance of load bearing cold-formed steel interior and exterior wall systems, *Thin-Walled Struct.* 73 (2013) 145–157, <https://doi.org/10.1016/j.tws.2013.07.017>.
- [24] M. Balarupan, Structural Behaviour and Design of Cold-formed Steel Hollow Section Columns under Simulated Fire Conditions (Doctor of Philosophy), School of Civil Engineering and Built Environment, Queensland University of Technology, Queensland, Australia, 2015.
- [25] S. Kesawan, M. Mahendran, Y. Dias, W.-B. Zhao, Compression tests of built-up cold-formed steel hollow flange sections, *Thin-Walled Struct.* 116 (2017) 180–193, <https://doi.org/10.1016/j.tws.2017.03.004>.
- [26] D. Simulia, ABAQUS Analysis User's Manual. (<https://classes.engineering.wustl.edu/2009/spring/mase5513/abaqus/docs/v6.6/books/stm/default.htm?startat=ch02s11ath45.html>), (Accessed 2020).
- [27] M. Rusthi, P. Keerthan, M. Mahendran, A. Ariyanayagam, Investigating the fire performance of LSF wall systems using finite element analyses, *J. Struct. Fire Eng.* 8 (4) (2017) 354–376, <https://doi.org/10.1108/jsfe-04-2016-0002>.
- [28] T. Suntharalingam, et al., Fire performance of innovative 3D printed concrete composite wall panels – a numerical study, *Case Stud. Constr. Mater.* 15 (2021), e00586, <https://doi.org/10.1016/j.cscm.2021.e00586>.
- [29] Eurocode 3: Design of steel structures – Part 1–2: General rules – Structural fire design, T. E. Union, 23 April 2004 2005.
- [30] H. Wang, Heat Transfer Analysis of Components of Construction Exposed to Fire (Ph.D.), Department of Civil Engineering and Construction, University of Salford, 1995. [Online]. Available: (<http://usir.salford.ac.uk/id/eprint/14780/>).
- [31] F. Liu, F. Fu, Y. Wang, Q. Liu, Fire performance of non-load-bearing light-gauge slotted steel stud walls, *J. Constr. Steel Res.* 137 (2017) 228–241, <https://doi.org/10.1016/j.jcsr.2017.06.034>.
- [32] V. Jatheeshan, M. Mahendran, Thermal performance of LSF floors made of hollow flange channel section joists under fire conditions, *Fire Saf. J.* 84 (2016) 25–39, <https://doi.org/10.1016/j.firesaf.2016.05.007>.
- [33] Eurocode 5: Design of timber structures – Part 1–2: General – Structural fire design, EN 1995-1-2:2004: E, T. E. Union, 2004.
- [34] D.I. Kolaitis, E.K. Asimakopoulou, M.A. Founti, Fire protection of light and massive timber elements using gypsum plasterboards and wood based panels: a large-scale compartment fire test, *Constr. Mater.* 73 (2014) 163–170, <https://doi.org/10.1016/j.conbuildmat.2014.09.027>.
- [35] M. Rusthi, A.D. Ariyanayagam, M. Mahendran, Fire design of LSF wall systems made of web-stiffened lipped channel studs, *Thin-Walled Struct.* 127 (2018) 588–603, <https://doi.org/10.1016/j.tws.2018.02.020>.
- [36] P. Santos, L. Silva, V. Ungureanu, Energy Efficiency of Lightweight Steel-framed Buildings. 2012.
- [37] P.C.R. Collier, A.H. Buchanan, Fire resistance of lightweight timber framed walls, *Fire Technol.* 38 (2) (2002) 125–145, <https://doi.org/10.1023/A:1014459216939>.
- [38] J. Schmid, J. Köhler, J. Köhler, Fire-exposed cross-laminated timber–modelling and tests, in: Proceedings of the World Conference on Timber Engineering, 2010.